

## Sensitive Determination of Anticancer Drug Methotrexate Using Graphite Oxide-Nafion Modified Glassy Carbon Electrode

Deqian Huang<sup>1,2,\*</sup>, Hai Wu<sup>1,2</sup>, Yuyang Zhu<sup>1,2</sup>, Huijuan Su<sup>1,2</sup>, Hong Zhang<sup>1,2</sup>, Liangquan Sheng<sup>1,2</sup>, Zhaodi Liu<sup>1,2</sup>, Huajie Xu<sup>1,2</sup>, and Chongfu Song<sup>1,2</sup>

<sup>1</sup> School of Chemistry and Material Engineering, Fuyang Normal University, Anhui, Fuyang, 236037, P. R. China

<sup>2</sup> Anhui Provincial Key Laboratory for Degradation and Monitoring of Pollution of The Environment, Fuyang Anhui 236037, P. R. China

\*E-mail: [huangdeqian@163.com](mailto:huangdeqian@163.com)

Received: 28 November 2018 / Accepted: 15 January 2019 / Published: 10 March 2019

In this paper, a graphite oxide-Nafion-glassy carbon electrode (GO-Nafion-GCE) by coating method was fabricated and used for study the electrochemical behavior and measurement of methotrexate (MTX) by cycle voltammetry (CV). The influence factors, such as volume of modifier, type of supporting electrolyte, concentration of electrolyte, scan rate, preconcentration time, and preconcentration potential on the anodic peak current of MTX were examined. The experimental results indicated that the electrode process is an adsorption-diffusion mixed controlled process. Under the experimental conditions of research, the anodic peak current of MTX shows a linear relationship within concentration range of  $4.0 \times 10^{-7}$ – $2.0 \times 10^{-5}$  mol L<sup>-1</sup>. The linear relationship can be expressed with the equation of  $I_{p,a}(\mu A) = (0.4739 \pm 0.0086)C(\mu M) + (0.2885 \pm 0.0434)$ . Under the optimum electrochemical experimental conditions, the limit of detection (LOD) can be calculated to be  $9.0 \times 10^{-9}$  mol L<sup>-1</sup> (S/N=3). The proposed method has been used for the detection of MTX in methotrexate injection and urine samples successfully.

**Keywords:** anticancer drug; methotrexate; graphite oxide-Nafion; determination

### 1. INTRODUCTION

Methotrexate (MTX), also named amethopterin or methylamineopterin, is a yellow anticancer drugs, which belongs to the category of folic acid and has analogy structure with folic acid [1–3]. It can inhibit the synthesis of tumour cells and inhibit the growth and reproduction of tumour cells by inhibiting the production of dihydrofolate reductase. Therefore, MTX is widely used for the remedy of some cancers, such as breast cancer [4], acute lymphoblastic leukemia [5], head and neck cancer [6],

lung cancer [7], malignant lymphoma [8], etc. However, due to its great toxic effect on cell rapid divisions, it can repress the growth and proliferation of noncancerous cells and lead to serious side effects containing myelosuppression [9], pulmonary fibrosis [10], interstitial pneumonia, small vasculitis and high teratogenicity [11,12]. Accordingly, the development of a simple, reliable, rapid, cheap and sensitive detection method for MTX is of great significance.

Several analytical strategies have been used for the determination of MTX, containing spectrophotometric [13], fluorimetry [14–16], capillary electrophoresis (CE) [17,18], ion chromatography (IC) [19], high performance liquid chromatography (HPLC) [20,21], and liquid chromatograph-mass spectrometer [22,23]. Although these methods have the superiorities in high sensitivity and high accuracy, they usually require cumbersome pretreatment or complex pre-separation procedures and lead to increase of the cost and time of detection [24]. However, electrochemical detection methods have been paid close attention in virtue of their advantages of cheapness, sensitivity, simplicity, accuracy and potential of on-spot application [25]. Based on this, electrochemical methods can provide rapid and sensitive analytical performance due to their relatively inexpensive of instruments and the potential of miniaturization for MTX determination [26]. Electrochemical behavior and the measurement of MTX were researched employing different sensors, including hanging mercury drop electrode (HMDE) [27,28] and silver solid amalgam electrode [26]. However, with the increasing awareness of environmental protection, the applications of mercury electrode were reduced due to its high toxicity. The determination of MTX were reported using various modified electrodes [29–38] by cyclic voltammetry (CV) [24,29], chronoamperometry (CA) [32], square wave voltammetry (SWV) [29,30,36,37], or differential pulse voltammetry (DPV) [24–26,31,32,34, 35,38] for MTX determination. Patel et al. [39] reviewed the determination of MTX based on bioanalytical methods.

Graphite oxide (GO), also called graphite acid, belongs to a part of carbon-based nanomaterials with layered structure. It has wide applications for adsorption materials [40], supercapacitor [41], sensors [42–44], and so on. GO is usually prepared by treated with strong acid and then oxidized by strong oxidant, for instance potassium permanganate [40,45]. The treated process enables GO to obtain hydroxyl, carboxyl and epoxides, and link to its layers by covalent bonding, which makes GO can extensively disperse in water [42]. The existence of these oxygen-containing functional groups can result in different polar substances be easily embedded between their layers, thus forming a graphite oxide intercalated composite [46].

Sulfonated tetrafluoroethylene (Nafion) is a fine ion exchange fluoropolymer, which has high chemical, electrochemical, thermal stability, and favourable biocompatibility of unique ionic properties [47], which has received a considerable attentions due to its application to fuel cells [48], electrochemical sensors [49–51], and so on.

In the present study, GO-Nafion-GCE was prepared and applied to the detection of MTX by CV method. The electrochemical analytical conditions were optimized. The interference experiment, repeatability experiment, and real sample analysis were also carried out using the developed modified electrode. The developed method has been applied to measure MTX in methotrexate injection and urine samples.

## 2. EXPERIMENTAL

### 2.1. Apparatus and reagents

The electrochemical experiment was performed with a CHI 660D electrochemical workstation (Chenhua Instruments in Shanghai, PR China). The conventional three-electrode system was employed for the whole electrochemical determination experiment, including a GO-Nafion-GCE or a bare GCE ( $d=3$  mm), a platinum wire auxiliary electrode (PWAE) and a saturated calomel reference electrode (SCE) [52], respectively. HPLC (Waters 1525, USA) with a UV/Vis detector (Waters 2489, USA) and a chromatographic column (WATERS 4.6×150 mm, 5  $\mu\text{m}$ ) at a wavelength of 306 nm was used for the determination of MTX. Other conditions were used as ref. [31].

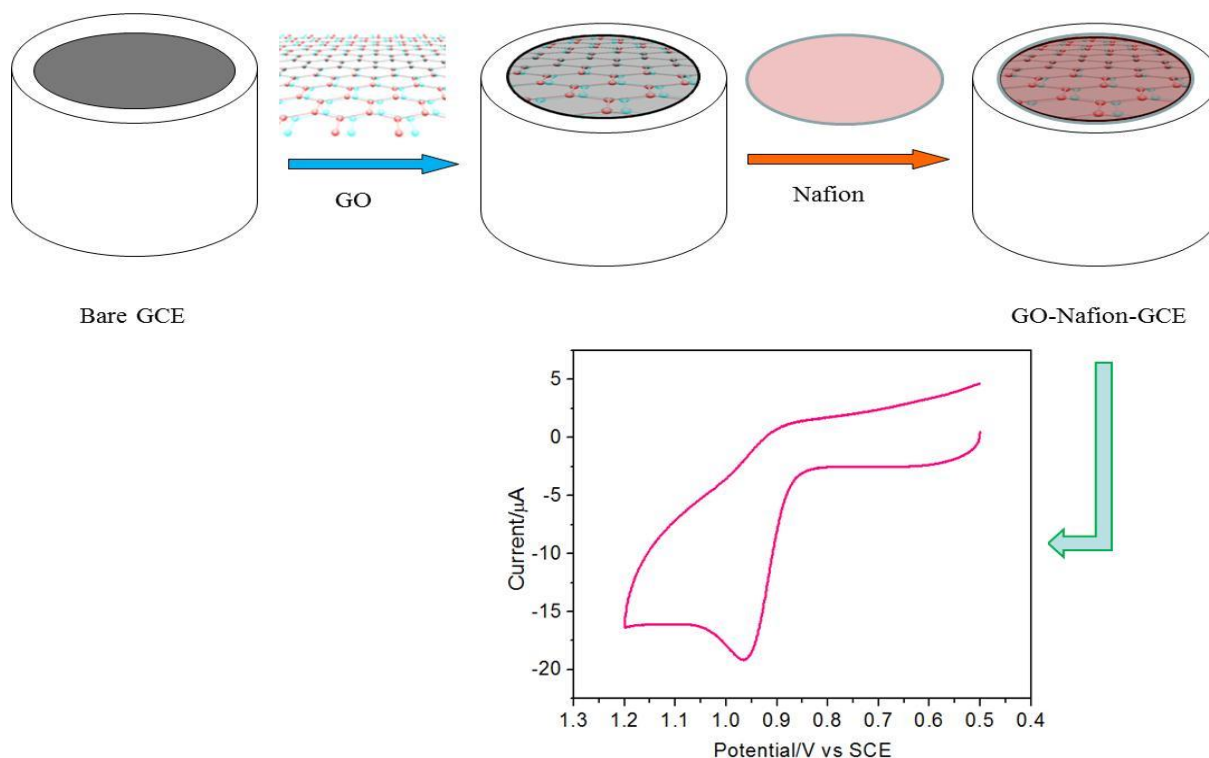
MTX (Aladdin reagent Co., Ltd., Shanghai, P.R. China) was prepared daily by dissolving of MTX in 0.1 mol L<sup>-1</sup> sodium hydroxide, and stocked at 4 °C of refrigerator. Methotrexate injection was obtained from Pfizer. NYSE: PFE. Other reagents (Shanghai Chemicals Co., Ltd., Shanghai, P.R. China) were at least of analytical reagent and used as received unless otherwise stated. All solutions were prepared in double deionized water. The whole experiments were in progress at approximately 25 °C.

### 2.2. Fabrication of graphite oxide

The preparation of GO was in accordance with the approach of reference [45]. The detailed procedures are as follows: 23 mL of concentrated sulphuric acid was cooled to about zero using ice water mixed bath, then 1 g of graphite powder and 3 g of potassium permanganate was added slowly under the condition of intense stirring and kept the temperature is not more than 20 °C. After mixing and homogenization, the mixture was put in the 35 °C water baths to react for 2 h, then 46 mL of double deionized water was added and maintained the system temperature was  $\leq 98$  °C and agitated for 15 min. After this, 140 milliliters of double deionized water and 10 milliliters of 30% H<sub>2</sub>O<sub>2</sub> were added in turn and filtered when it is still hot. The filter cake was washed until SO<sub>4</sub><sup>2-</sup> was not detected in the filtrate using 1 mol L<sup>-1</sup> of HCl, and then washed to neutral with double deionized water, afterwards the sample was desiccated under conditions of vacuum for 12 hours.

### 2.3. Fabrication of GO-Nafion-GCE

1.0 milligram of GO was dispersed into 1 milliliter of 10% Nafion-ethanol (v/v) solution with the assist of ultrasonic for 1 h until a 1 mg mL<sup>-1</sup> homogeneous mixed solution was obtained. Beforehand of modification, the bare GCE was finished on a polishing cloth utilizing 0.05  $\mu\text{m}$  alumina slurry, then rinsed completely using double deionized water and sonicated in a mixture solution of ethanol and water of 1:1 (v/v) for 5 min. After this, the homogeneous mixed solution of GO-Nafion was dropped onto GCE surface and dried in air. Afterwards the GO-Nafion-GCE was scanned at the scan rate of 100 mV s<sup>-1</sup> from 0.5 to 1.2 V in 0.03 mol L<sup>-1</sup> perchloric acid until a stable cyclic voltammetric curve obtained. The fabrication of GO-Nafion-GCE and the determination procedure for MTX are illustrated with Scheme 1.



**Scheme 1.** Schematic diagram of GO-Nafion-GCE preparation process and determination of MTX.

#### 2.4. Procedure

10 milliliter of supporting electrolyte and a given volume of MTX standard solution or real samples were mixed uniformly in an electrolyte cell, and the cyclic voltammograms were recorded in the range of 0.5–1.2 V under the conditions of concentration. The concentration of MTX was calculated through the  $I_p$  of MTX in the absence and presence of MTX. The data was processed with Excel 2010 and Origin 6.0 software.

### 3. RESULTS AND DISCUSSION

#### 3.1 The electrochemical behavior of MTX

The CV behavior of MTX was researched using bare GCE and GO-Nafion-GCE. It can be seen (Fig. 1) that there is an anodic peak both at a bare GCE and at GO-Nafion-GCE surface between 0.5 V and 1.2 V. There is no corresponding cathode peak at the reverse scan, which indicates that the electrochemical reaction of MTX is an irreversible electrode process at both the bare electrode and GO-Nafion-GCE. The anodic peak current is significantly improved at the GO-Nafion-GCE in comparison with that at a bare GCE. Furthermore, the peak potential of MTX is negative shifted about 80 mV at the GO-Nafion-GCE (1.044V) surface compared with that at a bare GCE (0.964V) surface. Obviously the transfer rate of electron is increased at the GO-Nafion-GCE, which is mainly attributed to the catalytic effect of GO-Nafion toward MTX [36]. The electrochemical response mechanism of MTX at the GO-Nafion-GCE is proposed as shown in scheme 2.

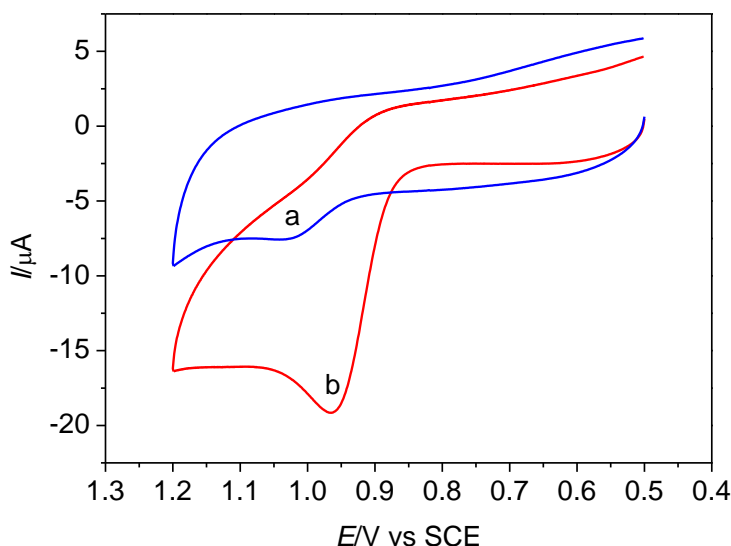
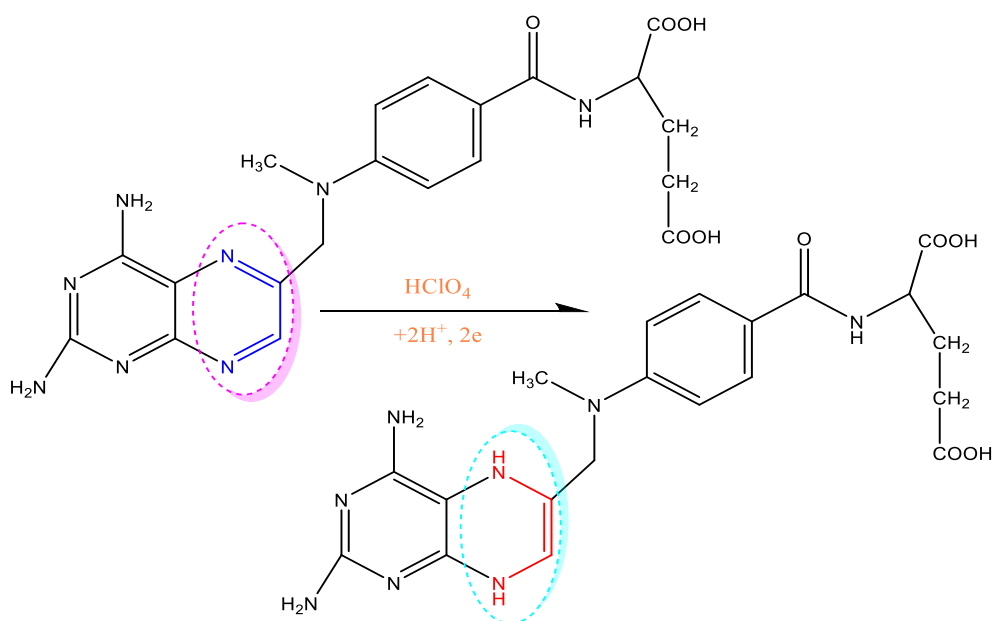


**Figure 1.** CV plots of methotrexate ( $5.0 \times 10^{-5} \text{ mol L}^{-1}$ ) at a bare GCE surface (a) and a GO-Nafion-GCE (b) in  $0.03 \text{ mol L}^{-1}$  perchloric acid at scan rate of  $0.1 \text{ V s}^{-1}$ . Preconcentration time: 120 s.



**Scheme 2.** Schematic illustration of electrochemical reaction mechanism of MTX at GO-Nafion-GCE surface.

### 3.2 Influence of supporting electrolyte

Several supporting electrolytes such as  $0.1 \text{ mol L}^{-1}$  perchloric acid, sulphuric acid, phosphate, and sodium hydroxide aqueous solution were investigated at GO-Nafion-GCE by CV method. It can be seen that well-defined CV responses of MTX were observed in  $0.1 \text{ mol L}^{-1}$  perchloric acid and sulphuric acid aqueous solutions, however, a higher CV peak current and well CV peak shape were obtained in  $0.1 \text{ mol L}^{-1}$  perchloric acid (Fig. 2). Thus, perchloric acid is selected as supporting electrolyte.

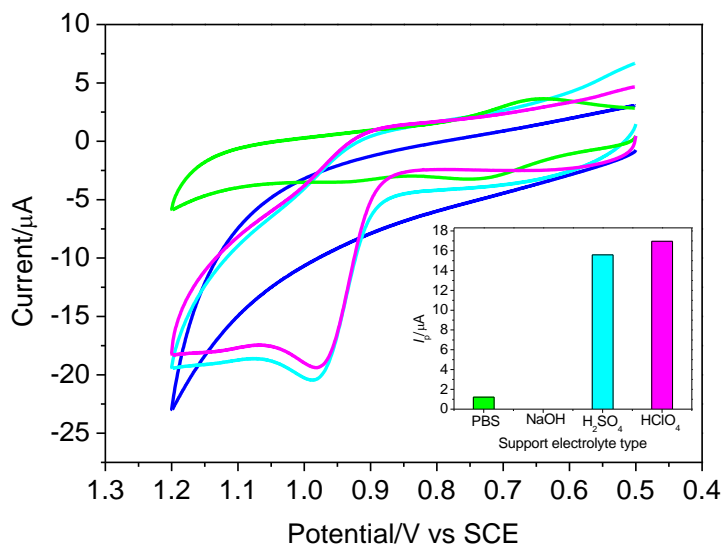


**Figure 2.** CV curves of MTX ( $5.0 \times 10^{-5} \text{ mol L}^{-1}$ ) in different supporting electrolytes. Inset: Bar graph between peak currents of MTX and the type of supporting electrolytes.

### 3.3 Influence of supporting electrolyte concentration

The effect of perchloric acid concentration on the CV peak current of MTX was researched. It can be seen clearly (Fig. 3) that the CV peak current is increased obviously with the addition of perchloric acid concentration, and the electrochemical response of MTX is maximizing as the concentration of perchloric acid is  $0.03 \text{ mol L}^{-1}$ . Therefore, the followed experiments were performed in  $0.03 \text{ mol L}^{-1}$  perchloric acid solution.

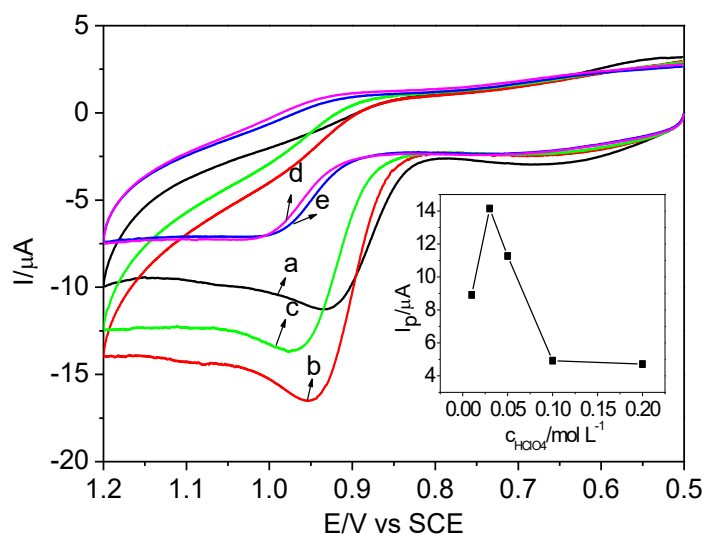


**Figure 3.** CV curves of MTX ( $5.0 \times 10^{-5} \text{ mol L}^{-1}$ ) in different concentrations of perchloric acid.  $c_{\text{HClO}_4}$ : 0.01, 0.03, 0.05, 0.1, and 0.2 mol L<sup>-1</sup>. Inset: The Plot of  $I_{p\text{MTX}}-c_{\text{HClO}_4}$ .

### 3.4. Influence of scan rate

In order to make further efforts to inspect the electrochemical reaction mechanism of MTX at the GO-Nafion-GCE surface, the impact of scan rate was investigated. Fig. 4 indicates the CV superposition graphs of MTX at different scan rates within 0.025–0.25 V s<sup>-1</sup>. Obviously, the oxidation peak currents are increased with enhancing of scan rates. However, the oxidation peak currents of MTX are neither increased linearly with scan rates nor with the square root of scan rates, which indicated that the electrode process is neither a diffusion-controlled process nor an adsorption-controlled process but by some kinetic reaction [25]. Fig.4A and inset indicate that the logarithm of anodic peak currents is linearly proportional to the logarithm of the scan rates between 0.025 and 0.25 V s<sup>-1</sup>, and the linear regression equation is  $\log(I_{pa}/\mu\text{A}) = 0.333\log(v/V \text{ s}^{-1}) + 1.40$  ( $r=0.9980$ ). According to the slope of regression equation, the result shows that the electrode process is a kinetic-controlled process by diffusion, which agreed with the result that at the boron-doped diamond electrode [25]. If the electrode process is an adsorption-diffusion mixed controlled process, the relationship between peak currents of MTX and scan rates can be presented with equation (1):

$$I_p/\mu\text{A} = k_1(v/V \text{ s}^{-1})^{1/2} + k_2(v/V \text{ s}^{-1}) + k_3 \quad (1)$$

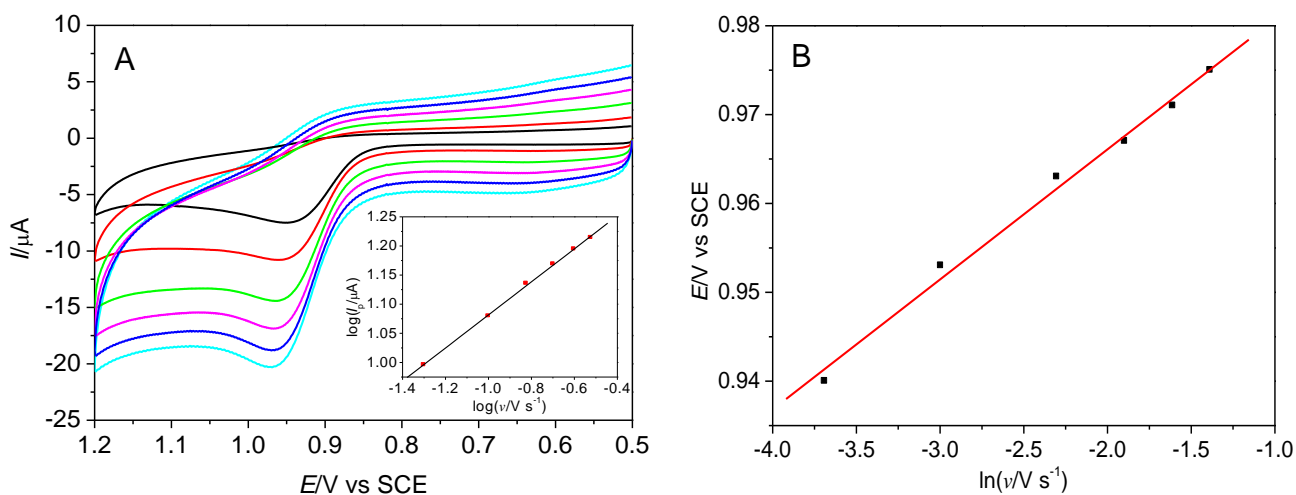


**Figure 4.** CV curves of MTX ( $5.0 \times 10^{-5}$  mol L<sup>-1</sup>) at different scan rates (A), and the plot between  $E_p$  and  $\ln v$  (B). Scan rate: 0.025, 0.05, 0.1, 0.15, 0.2, 0.25 V s<sup>-1</sup>. Buffer: 0.03 mol L<sup>-1</sup> perchloric acid. Inset A: The plot between  $\log I_p$  of MTX and  $\log v$ .

Through the regression analysis of Excel,  $k_1 = 44.2$  ( $P=0.00048$ ),  $k_2 = -30.2$  ( $P=0.000045$ ) and  $k_3 = 1.07$  ( $P=0.0096$ ) can be obtained with a correlation coefficient of 0.9999, respectively. By substituting the above coefficient into equation (1), the regression equation  $I_p/\mu\text{A} = 44.2(v/V \text{ s}^{-1})^{1/2} - 30.2(v/V \text{ s}^{-1}) + 1.07$  can be obtained, which further demonstrates that the oxide process is an adsorption-diffusion mixed controlled process [53].

The effect of scan rates on the peak potentials of MTX was also considered using GO-Nafion-GCE. It is clearly (Fig. 4B) that the  $E_p$  shows a linear relationship with  $\ln v$  as the scan rates between 0.025 V s<sup>-1</sup> and 0.25 V s<sup>-1</sup>. The linear regression equation is  $E_{pa} = 0.0146\ln v + 0.995$ ,  $r=0.9957$ , which affirms that the electrode process is an irreversible electrode process. For an irreversible electrode

processes controlled by adsorption, the relationship between  $E_{pa}$  and  $\nu$  can be expressed by Laviron's equation.

$$E_{pa} = E^{\circ} - \frac{RT}{\alpha nF} \ln \frac{RTk_s}{\alpha nF} + \frac{RT}{\alpha nF} \ln \nu \quad (2)$$

Where  $E^{\circ}$  is formal standard potential,  $\alpha$  is charge transfer coefficient,  $n$  is electron transfer numbers, and  $k_s$  is standard electron transfer rate constant.  $R$ ,  $T$  and  $F$  have their common meaning. on the basis of the slope and the intercept of  $E_p=0.0461\ln\nu + 0.995$ , the straight line of peak potential ( $E_p$ ) against  $\ln\nu$  of equation (2),  $\alpha n = 1.60$  can be gained. The number of electrons involved in the electrode process can be counted according to the equation (3).

$$I_p = \frac{n^2 F^2 \Gamma A \nu}{4RT} = \frac{nFQ\nu}{4RT} \quad (3)$$

$I_p$ ,  $\Gamma$ ,  $A$ , and  $Q$  are peak current (amperes) of MTX, the total concentration of reaction substance ( $\text{mol}\cdot\text{cm}^{-2}$ ), the electrode area ( $\text{cm}^2$ ), and the peak area of cyclic voltammogram (coulomb), respectively.  $F$  is the Faraday constant, and  $n$  is the number of electrons transferred.  $R$  and  $T$  have the same meanings as equation (2). The equation (3) demonstrates that the electron transfer numbers  $n$  can be computed provided  $Q$  is gained at a certain scan rate. The relationship between  $I_p$  and  $\nu$  is in accord with equation (1) within  $0.025\text{--}0.25 \text{ V s}^{-1}$ , meaning that the peak currents of MTX is not only related with scan rate but also the square root of scan rate. However, the electron transfer number ( $n$ ) was calculated as 1.63, 1.53, 1.59, 1.54, 1.51 and 1.70 as the scan rates are 0.025, 0.05, 0.1, 0.15, 0.2 and  $0.25 \text{ V s}^{-1}$ , respectively, indicating that  $2e$  was involved. Hence,  $\alpha=0.88$  can be obtained. Identically,  $E^{\circ}=0.937 \text{ V}$  can be gained from the intercept of  $E_p$  versus  $\nu$  plot on longitudinal coordinates by extrapolating the line to be  $\nu = 0$  [37], and the value of  $k_s$  of  $1.29 \text{ s}^{-1}$  was counted accordance with the intercept of the straight line of  $E_p\text{--}\ln\nu$ .

### 3.5. Influence of concentration potential

The effect of accumulation potential on the oxidation peak current of MTX ( $5.0 \times 10^{-5} \text{ mol L}^{-1}$ ) was performed. The results demonstrated that the accumulation potential has a little effect as the accumulation potentials between  $-0.2$  and  $0.2 \text{ V}$ . At more positive or negative potentials, a decrease of anodic peak current was observed. Thus, the determination of MTX was accumulated under the condition of open circuit.

### 3.6. Influence of concentration time

Accumulation is generally an effective means to augment the peak current of determination. The impact of concentration time on the  $I_p$  of MTX ( $5.0 \times 10^{-5} \text{ mol L}^{-1}$ ) was investigated. The peak current of MTX is enhanced gradually with increasing of concentration time, and it reached maximum as the concentration time is 120 s. Thus, 120 s was adopted for subsequent determination of MTX.



### 3.7. Repeatability and detection limit

For the sake of inspecting the repeatability of the GO-Nafion-GCE, the experiments of repeatability were performed in 0.03 mol L<sup>-1</sup> perchloric acid. The RSD ( $n=8$ ) is 0.8 % for  $5.0 \times 10^{-5}$  mol L<sup>-1</sup> of MTX, which indicates that the GO-Nafion-GCE exhibits good repeatability. The limit of detection (LOD) is  $9.0 \times 10^{-9}$  mol L<sup>-1</sup> (LOD=3S/N).

### 3.8. Interference experiment

For the potential analytical application of the GO-nafion-GCE, the influence of various interfere species that possible existence in biological samples were assessed for 50  $\mu$ mol L<sup>-1</sup> of MTX. The tolerance times of foreign species were considered as interference provided the electrochemical signal ( $I_p$ ) of MTX arising a relative error  $> \pm 5\%$ . The results of the interference test are shown in Table 1. All the results suggested that the GO-Nafion-GCE has high selectivity for determination of MTX.

**Table 1.** Maximum tolerable times for  $5.0 \times 10^{-5}$  MTX of some interferents.

Interferents	Tolerable interference times
Na <sup>+</sup> , K <sup>+</sup> , Zn <sup>2+</sup> , Mg <sup>2+</sup> , Ca <sup>2+</sup> , Fe <sup>3+</sup>	500
Fe <sup>2+</sup>	120
Cl <sup>-</sup> , SO <sub>4</sub> <sup>2-</sup> , NO <sub>3</sub> <sup>-</sup> , CO <sub>3</sub> <sup>2-</sup> , Ac <sup>-</sup>	500
Oxalic acid, glucose, sucrose, citric acid, tartaric acid, uric acid	400
Ascorbic acid	50

### 3.9. Calibration curve

Fig. 5 shows the CV superposition figures of different concentrations of MTX. Obviously, the anodic peak current of MTX is enhanced gradually with increasing of MTX concentration. The anodic peak current shows a linear relationship with MTX concentration from  $4.0 \times 10^{-7}$  to  $2.0 \times 10^{-5}$  mol L<sup>-1</sup> with a linear regression equation of  $I_{p,a}(\mu A) = (0.4739 \pm 0.0086)C (\mu M) + (0.2885 \pm 0.0434)$  ( $r = 0.9985$ ). The limit of detection (LOD) can be calculated as  $9.0 \times 10^{-9}$  mol L<sup>-1</sup> according to  $LOD = 3s_b/N$  defined by IUPAC [7], which is more lower than that at some of modified electrodes as indicated in Table 2, similar to that at DNA Langmuir–Blodgett modified GCE [29], DNA/SWCNT/Nafion GCE [37], and higher than at AgSAE [26] and bismuth film modified electrode [34] and. But, compared with other modified electrode, the proposed electrochemical method in our work owns the advantages of cheap, high sensitivity, simplicity, and good stability.

### 3.10. Determination of MTX in methotrexate injection and urine

Under the selected conditions, the GO-Nafion-GCE was used to measure MTX in methotrexate injection and urine by standard addition method. The determination steps are as follows: a given volume of methotrexate injection or urine was transferred using a microinjector and added into 10 mL 0.03 mol L<sup>-1</sup> perchloric acid solution. After the solution was mixed, the CV curves were recorded, and then different volumes MTX standard solution was added. The total MTX concentration detected in methotrexate injection is 24.86 ± 0.23 mg mL<sup>-1</sup>, and in accordance with the nominal content of 50 mg 2 mL<sup>-1</sup>. The results were compared with that obtained by HPLC ( $\alpha=0.05$ ) in the case described in Apparatus and reagents section (Table 3), which indicated that the proposed method is reliable in the determination of MTX in methotrexate injection and urine.

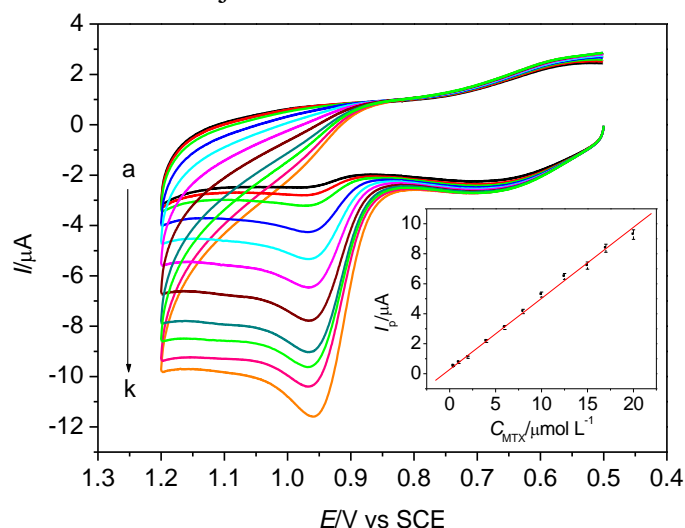


**Figure 5.** CV curves changed with MTX concentration. Buffer: 0.03 mol L<sup>-1</sup> perchloric acid. Scan rate: 0.1 V s<sup>-1</sup>. Inset: The linear relationship between current responses and MTX concentration. a→k: 0.4, 1.0, 2.0, 4.0, 6.0, 8.0, 10, 12.5, 15, 17, and 20 μmol L<sup>-1</sup>.

**Table 2.** Comparison of GO-Nafion-GCE with other sensors for the determination of MTX.

Modified electrode	Methods	Linear range (mol L <sup>-1</sup> )	LOD (mol L <sup>-1</sup> )	Ref.
3DPG-CNT/GCE	CV, DPV	$7.0 \times 10^{-7}$ – $1.0 \times 10^{-4}$	$7.0 \times 10^{-8}$	[24]
BDDE	DPV	$5.0 \times 10^{-8}$ – $2.0 \times 10^{-5}$	$1.0 \times 10^{-8}$	[25]
AgSAE	DPV	$2.0 \times 10^{-9}$ – $1.0 \times 10^{-6}$	$1.8 \times 10^{-9}$	[26]
DNA /GCE(OX)	SWV	$2.0 \times 10^{-8}$ – $4.0 \times 10^{-6}$	$5.0 \times 10^{-9}$	[29]
Activated-GCE	SWV	$2.0 \times 10^{-6}$ – $3.6 \times 10^{-6}$	$1.0 \times 10^{-8}$	[30]
MWCNTs-DHP/GCE	DPAdSV	$5.0 \times 10^{-8}$ – $5.0 \times 10^{-6}$	$3.3 \times 10^{-8}$	[31]
WP/N-CNT-SPE	DPV, CV, CA	$1.0 \times 10^{-8}$ – $5.4 \times 10^{-4}$	$4.5 \times 10^{-8}$	[32]
BiFE	DPAdSV	$1.2 \times 10^{-8}$ – $1.65 \times 10^{-6}$	$9.0 \times 10^{-10}$	[34]
CD-GNs/GCE	DPV	$1.0 \times 10^{-7}$ – $1.0 \times 10^{-6}$	$2.0 \times 10^{-8}$	[35]
nano-Au/MWNTs-ZnO-SPE	SWASV	$2.0 \times 10^{-8}$ – $1.0 \times 10^{-6}$	$5.63 \times 10^{-9}$	[36]
DNA/SWCNT/Nafion GCE	SWASV	$2.0 \times 10^{-8}$ – $1.5 \times 10^{-6}$	$8.0 \times 10^{-9}$	[37]
PABSA/Q-MWNTs/GCE	DPV	$1.0 \times 10^{-7}$ – $8.0 \times 10^{-6}$	$1.5 \times 10^{-8}$	[38]

GO-Nafion-GCE	CV	$4.0 \times 10^{-7}$ – $1.5 \times 10^{-5}$	$9.0 \times 10^{-9}$	This work
---------------	----	---	----------------------	-----------

SPE: screen-printed electrode; 3DPG-CNT: 3D porous graphene-carbon nanotube; BDDE: boron-doped diamond electrode; m-AgSAE: silver solid amalgam electrode; DHP: dihexadecyl hydrogen phosphate; BiFE: Bismuth film modified electrode; CD-GNs: Cyclodextrin-graphene hybrid nanosheets; nano-Au/LC: Nano-Au/L-cysteine; PABSA/Q: p-aminobenzene sulfonic acid/quaternary amine; PSA: Potentiometric stripping analysis; ABSA: p-aminobenzene sulfonic acid.

**Table 3.** Determination results of MTX in methotrexate injection and urine ( $n=3$ ).

Sample	Detected ( $\mu\text{mol L}^{-1}$ )	Comparative method ( $\mu\text{mol L}^{-1}$ )	Added ( $\mu\text{mol L}^{-1}$ )	Found ( $\mu\text{mol L}^{-1}$ )	Recovery (%)
Injection 1	10.23	10.16	5.00	15.41	103.6
Injection 2	10.18	10.13	10.00	20.36	101.8
Injection 3	10.06	10.11	15.00	24.84	98.5
Urine 1	–	–	5.00	5.13	102.6
Urine 2	–	–	10.00	10.38	103.8
Urine 3	–	–	15.00	14.55	97.0

–No found

#### 4. CONCLUSIONS

In the present work, GO-Nafion-GCE was prepared and applied to determine MTX in methotrexate injection and urine successfully. The GO-Nafion modified GCE was extremely appropriate and effective for MTX determination in real samples. The recoveries are from 97.0 % to 103.8 % using the proposed method. Since GO-Nafion-GCE provides a cheap and appreciable repeatability, it may offer a potential on-spot application for clinical diagnosis.

#### ACKNOWLEDGEMENTS

This work is supported by Natural Science Foundation of Colleges and Universities in Anhui Province (2014KJ024), Fuyang Municipal Government -- Fuyang Normal College Horizontal Cooperation Major Project (XDHX201701) and Key Project (XDHX2016009), Innovation Team of Modern Analytical Technologies (kytd201701), and State Key Laboratory of Analytical Chemistry for Life Science (SKLACLS1712).

#### References

1. S. Farber, L.K. Diamond, R.D. Mercer, R.F. Sylvester and J.A. Wolff, *N. Engl. J. Med.*, 238 (1948) 787–793
2. M. Levitt, M.B. Mosher, R.C. Deconti, L.R. Farber, R.T. Skeel, J.C. Marsh, M.S. Mitchell, R.J. Papac, E.D. Thomas and J.R. Bertino, *Cancer Res.*, 33 (1973) 1729–1734.
3. T. Sakura, F. Hayakawa, I. Sugiura, T. Murayama, K. Imai, N. Usui, S. Fujisawa, T. Yamauchi, T. Yujiri and K. Kakihana, *Leukemia*, 32 (2018) 626–632.

4. H.K. Ahn, B. Han, S.J. Lee, T. Lim, J.M. Sun, J.S. Ahn, M.J. Ahn and K. Park, *Lung Cancer*, 76 (2012) 253–254.
5. D. Cameron, J.P. Morden, P. Canney, G. Velikova, R. Coleman, J. Bartlett, R. Agrawal, J. Banerji, G. Bertelli and D. Bloomfield, *Lancet Oncol.*, 18 (2017) 929–945.
6. H. Park, D.H. Yoon, Y. Song, H. Kim, Y. Huh, S. Kim, S. Jang, C.J. Park, H.S. Chi, C.S. Park, J. Huh, S.W. Lee and C. Suh, *Blood*, 118 (2011) 698–699.
7. E.E. W. Cohen, L.F. Licitra, B. Burtness, J. Fayette, T. Gauler, P.M. Clement, J.J. Grau, J.M. del Campo, A. Mailliez and R.I. Haddad, *Ann. Oncol.*, 28 (2017) 2526–2532.
8. J.T. Sandlund, C.H. Pui, H. Mahmoud, Y. Zhou, E. Lowe, S. Kaste, L.E. Kun, M.J. Krasin, M. Onciu, F.G. Behm, R.C. Ribeiro, B.I. Razzouk, S.C. Howard, M. L. Metzger, G.A. Hale, R. Rencher, K. Graham and M.M. Hudson, *Ann. Oncol.*, 22 (2011) 468–471.
9. X.N. Wei, D.H. Zheng, Y.O. Mo, J.D. Ma, Y.L. Chen and L. Dai, *Ann. Rheum. Dis.*, 76 (2017) 279–280.
10. M. Ohbayashi, S. Kubota, A. Kawase, N. Kohyama, Y. Kobayashi and T. Yamamoto, *J. Toxicol. Sci.*, 39 (2014) 319–330.
11. J.E. Gach, R.A. Sabroe, M.W. Greaves and A.K. Black, *Br. J. Dermatol.*, 145 (2001) 340–343.
12. D.M. Sandoval, G.S. Alarcon and S.L. Morgan, *Br. J. Rheumatol.*, 34 (1995) 49–56.
13. C.S.P. Sastry and J. Rao, *Anal. Lett.* 29 (1996) 1763–1778.
14. S. Chen, Z. Zhang, D. He, Y. Hu and H. Zheng, *Luminescence*, 22 (2007) 338–342.
15. S.M. Chen and Z.J. Zhang, *Spectrochim. Acta A*, 70 (2008) 36–41.
16. A. Espinosa-Mansilla, I. Durán Merás, A. Zamora Madera, L. Pedano and C. Ferreyra, *J. Pharm. Biomed. Anal.*, 29 (2002) 851–858.
17. Z. Szakacs and B. Noszai, *Electrophoresis*, 27 (2006) 3399–3409.
18. J. Rodriguez Flores, G. Castaneda Penalvo, A. Espinosa Mansilla and M.J. Rodriguez Gomez, *J. Chromatogr. B*, 819 (2005) 141–147.
19. Z.Y. Zhu, H.W. Wu, S.C. Wu, Z.P. Huang, Y. Zhu and L.L. Xi, *J. Chromatogr. A*, 1283 (2013) 62–67.
20. S.P. Fang, C.P. Lollo, C. Derunes and M.J. LaBarre, *J. Chromatogr. B*, 879 (2011) 3612–3619.
21. K. Michaila and M.S. Moneeb, *J. Pharm. Biomed. Anal.*, 55 (2011) 317–324.
22. D. Wu, Y.X. Wang, Y. Sun, N. Ouyang and J. Qian, *Biomed. Chromatogr.*, 29 (2015) 1197–1202.
23. I. Rodin, A. Braun, A. Stavrianidi and O. Shpigun, *J. Chromatogr. B*, 937 (2013) 1–6.
24. E. Asadian, S. Shahrokhian, A.I. Zad and F. Ghorbani-Bidkorbeh, *Sens. Actuators B*, 239 (2017) 617–627.
25. R. Selesovsk, L. Jankov-Bandzuchov and J. Chylkov, *Electroanalysis*, 27 (2015) 42–51.
26. R. Selesovska, L. Bandzuchova and T. Navratil, *Electroanalysis*, 23 (2011) 177–187.
27. J. Wang, P. Tuzhi, S. Meng and T. Tapia, *Talanta*, 33 (1986) 707–712.
28. B.X. Ye, S. Qu, F. Wang and L. Li, *J. Chin. Chem. Soc.*, 52 (2005) 1111–1116.
29. F. Wang, Y.J. Wu, J.X. Liu and B.X. Ye, *Electrochim. Acta*, 54 (2009) 1408–1413.
30. L. Gao, Y.J. Wu, J.X. Liu and B.X. Ye, *J. Electroanal. Chem.*, 610 (2007) 131–136.
31. G.G. Oliveira, B.C. Janegitz, V. Zucolotto and O. Fatibello-Filho, *Cent. Eur. J. Chem.*, 11 (2013) 1837–1843.
32. H.F. Zhou, G.X. Ran, J.F. Massonb, C. Wang, Y. Zhao and Q.J. Song, *Biosens. Bioelectron.*, 105 (2018) 226–235.
33. S. Phal, B. Lindholm-Sethson, P. Geladi, A. Shchukarev and S. Tesfalidet, *Anal. Chim. Acta*, 987 (2017) 15–24.
34. D. Asbahr, L.C.S. Figueiredo-Filho, F.C. Vicentini, G.G. Oliveira, O. Fatibello-Filho and C.E. Banks, *Sens. Actuators B*, 188 (2013) 334–339.
35. Y. J. Guo, Y.H. Chen, Q. Zhao, S.M. Shuang and C. Dong, *Electroanalysis*, 23 (2011) 2400–2407.
36. Y.T. Wang, J. Xie, L. Tao, H. Tian, S. Wang and H. Ding, *Sens. Actuators B*, 204 (2014) 360–367.

37. Y.W. Wang, H. Liu, F. Wang and Y.M. Gao, *J. Solid State Electrochem.*, 16 (2012) 3227–3235.
38. Z.Y. Zhu, F.L. Wang, F.M. Wang and L.L. Xi, *J. Electroanal. Chem.*, 708 (2013) 13–19.
39. H. Patel, P. Giri, A. Ghoghari, P. Delvadia, M. Syed and N. R. Srinivas, *Biomed. Chromatogr.*, 31 (2017) e3849–e3869.
40. M. Seredych, J.A. Rossin and T.J. Bandosz, *Carbon*, 49 (2011) 4392–4402.
41. B. Sidhureddy, A.R. Thirupathi and A.C. Chen, *Chem. Commun.*, 53 (2017) 7828–7831.
42. X.Q. Cui, X. Fang, H. Zhao, Z.X. Li and H.X. Ren. *Anal. Methods*, 9 (2017) 5322–5332.
43. N. Zeinali, M. Ghaedi and G. Shafie. *J. Ind. Eng. Chem.*, 20 (2014) 3550–3558.
44. R. Jain, A. Sinha, N. Kumari and A.L. Khan, *Anal. Methods*, 8 (2016) 3034–3045.
45. W.S. Hummers and R.E. Offeman, *J. Am. Chem. Soc.*, 80 (1958) 1339–1339.
46. K. Zhang, V. Dwivedi, C. Chi and J. Wu, *J. Hazard. Mater.*, 182 (2010) 162–168.
47. Z. Fan and D.J. Harrison, *Anal. Chem.*, 64 (1992) 1304–1311.
48. Y.X. Li, L. Liang, C.P. Liu, Y. Li, W. Xing and J.Q. Sun, *Adv. Mater.*, 30 (2018) 1707146.
49. Y. Yin, H. Wang and G. Liu, *Int. J. Electrochem. Sci.*, 13 (2018) 10259–10273.
50. J.Y. Jiang, Q.Y. Li, W.C. Wang, X.H. Chen and Z.D. Chen, *Int. J. Electrochem. Sci.*, 13 (2018) 587–597.
51. P.K. Kalambate, B.J. Sanghavi, S.P. Karnac and A.K. Srivastava, *Sens. Actuators B*, 213 (2015) 285–294.
52. D.Q. Huang, C. Chen, Y.M. Wu, H. Zhang, L.Q. Sheng, H.J. Xu and Z.D. Liu, *Int. J. Electrochem. Sci.*, 7 (2012) 5510–5520.
53. A.Y. Tesio, S.N. Robledo, H. Fernandez and M.A. Zon, *Bioelectrochem.*, 91 (2013) 62–69.
54. E.M. Maza, M.B. Moressi, H. Fernandez and M.A. Zon, *J. Electroanal. Chem.*, 675 (2012) 11–17.

© 2019 The Authors. Published by ESG ([www.electrochemsci.org](http://www.electrochemsci.org)). This article is an open access article distributed under the terms and conditions of the Creative Commons Attribution license (<http://creativecommons.org/licenses/by/4.0/>).